JOURNAL OF SOLID STATE CHEMISTRY 3, 89–100 (1971)

The Structure of the Bronze $Na_{13}Nb_{35}O_{94}$ and the Geometry of Ferroelectric Domains

D. C. CRAIG AND N. C. STEPHENSON

Department of Crystallography, School of Chemistry, University of New South Wales, Australia

Received August 3, 1970

The composition and structure of the oxide $Na_{13}Nb_{35}O_{94}$ has been determined from single crystal X-ray diffraction data. The unit cell is based on three tetragonal-bronze subcells in which all four- and five-sided tunnels are filled with interstitial ions. The niobium atoms exhibit square pyramidal, octahedral and pentagonal bipyramidal coordination while sodium ions, in the main, have square or trigonal prismatic coordination.

The space group is polar, *Pba2*, and each niobium atom is displaced from its basal octahedral plane by up to 0.12 Å in the same direction along [001]. The domain structure and orientation of domain boundaries, as revealed by electron transmission micrographs, are explained in terms of a reversal of polarity of adjacent ferroelectric domains.

Introduction

The system Na_2O–Nb_2O_5 has been examined by different workers and a number of stable phases have been reported together with suggested compositions. The only single crystal X-ray study in this system was carried out by Andersson (*1*) who described the structure of $NaNb_{13}O_{33}$, which differs slightly in composition from that originally given to it by Reisman et al. (*2*), viz., $Na_2Nb_{28}O_{71}$.

The compound $Na_2Nb_8O_{21}$ was described by Reisman et al. (*2*) and Shafer and Roy (*3*) as having an orthorhombic unit cell with $a = 12.39$, $b = 36.98$, and $c = 3.97$ Å. Andersson (*4*) reported this compound as $NaNb_3O_8$ and suggested that the structure is based upon that of the tetragonal tungsten-bronzes (T.T.B.). Whiston and Smith (*5*) came to a similar conclusion but preferred the composition to be $Na_{10}Nb_{34}O_{90}$ in order to give better agreement with the observed density of 4.62 gcm^{-3} ($\rho_c = 4.5$ gcm^{-3}).

In view of our interest in the T.T.B. structures (*6–8*) crystals of "$NaNb_3O_8$" were very kindly provided by Dr. Sten Andersson and we describe below the crystal structure determination, final composition, and domain structure of this compound.

Experimental

The "$NaNb_3O_8$" as obtained was in the form of irregular fragments, so to facilitate absorption correction it was reduced to spheres. Twinning is particularly common, on the [130] axis, and consequently it was necessary to examine several spheres by the Weissenberg method before a suitable one was found. The selected crystal, radius 0.04 mm, was transferred to a quartz fibre, and mounted on a specially designed arcless goniometer head.

A Siemens A.E.D. four-circle automatic diffractometer was used for data collection, crystal orientation and angle calculation being accomplished using the method of Busing and Levy (*9*). Cell dimensions were determined from selected high angle reflections, which were used also in the refinement of the approximate UB matrix.

Integrated intensities were obtained with CuK_α radiation, using a θ–2θ scan and the "five value method" (*10*) of measurement. The scan range varied from 1° at low theta to 2.5° at theta of 70°, the limit of the diffractometer.

The scan rate is controlled by the instrument, varying from 6 sec/deg for very intense reflections to a maximum set in this case at 60 sec/deg for the weak reflections. In addition, attenuation filters are automatically inserted when necessary to keep the count rate within the linear range of the equipment.

Intensities were corrected for instrumental drift, if any, using a periodically measured standard reflection as a reference. Background was assumed to vary linearly through the scan range for each reflection, and corrections for this, Lorentz polarization and absorption were applied using programmes written in this laboratory. Standard deviations were

assigned on the basis of counting statistics. A reflection was considered to be unobserved if its net intensity was less than 3σ, and its intensity was then assigned as 3σ.

The crystallographic data are

$Na_{13}Nb_{35}O_{94}$	F.W. 5054.5	
$a = 12.364(1)$,	$b = 36.992(4)$,	$c = 3.955(1)$
$V = 1808.9$ Å^3	$\mu R = 1.97$	S.G. *Pba*2
$\rho_0 = 4.62$	$\rho_c = 4.64$	

Structure Determination

The tetragonal tungsten bronze structure, as deduced by Magneli (*11*) for the phase K_xWO_3 ($0.48 < x < 0.54$), can be viewed as a two-dimensional network of corner-sharing octahedra which extends in a third direction again by corner sharing. This network contains three-, four-, and five-sided tunnels which can be filled in varying ways by metal and oxygen atoms. This process gives rise to compounds which have superlattices built upon the tetragonal tungsten-bronze subcell.

The compound "$NaNb_3O_8$" has a distribution of intensities and also unit-cell dimensions which indicate that the basic bronze subcell is tripled along the [010] direction. Ideal positions for the octahedrally coordinated metal atoms (niobium) were therefore calculated. The space group *Pba*2 was chosen in keeping with the polar nature of the T.T.B. structures and metal atoms in the general position 4*c* were each displaced 0.1 Å in the same direction away from the (002) plane. Least-squares refinement cycles were run in which $\Sigma W[|F_0| - |F_c|]^2$ values were minimised and, after convergence, these were followed by difference Fourier syntheses. In this way atoms were gradually located and their atomic parameters refined by utilising them in the F_c calculations. For these calculations the atomic form factors for O^{-2} and for Nb^{5+} and Na^+ were taken from Suzuki (*12*) and Cromer and Waber (*13*), respectively, and corrections for the real component of the anomalous dispersion of CuK_α by nobium were made with the $\Delta f'$ values given by Dauben and Templeton (*14*). Calculations were performed on an IBM 360/50 digital computer using programmes developed in this laboratory and local versions of ORFLS (*21*) and ORFFE (*21*).

As the refinement neared completion it became evident that all octahedrally coordinated metal atoms were niobium atoms. Population parameters did not significantly deviate from unity when Nb^{5+} atomic scattering curves were used for their F_c contribution. Also, 4 (symmetry related) five-sided tunnels were completely filled with niobium and oxygen atoms, giving these niobium atoms pentagonal bipyramidal coordination. Each of the 6 four-sided tunnels were filled with sodium atoms since the use of the f_{Na^+} curve for these atoms yielded normal temperature factors and population parameters of unity from the least-squares refinement cycles. The remaining 8 five-sided tunnels each contained some measure of electron density and from each surrounding oxygen atom environment it was evident that cations were to be located at these sites.

The composition of the unit cell, from the above considerations, is $Na_6Nb_{34}O_{94}$, leaving a total of 12 positive charges to be distributed over the 8 five-sided tunnels. Therefore, twelve sodium ions cannot be accommodated and the remaining choices are $Nb^{5+} + 7Na^+$ and $2Nb^{5+} + 2Na^+$ which give overall compositions of $Na_{13}Nb_{35}O_{94}$ and $Na_8Nb_{36}O_{94}$, respectively.

The correct composition was determined in the following manner. Four of the 8 five-sided tunnels of unknown occupancy contain single peaks in the difference Fourier synthesis. The remaining four have triplets; groups of three peaks each separated by ≈ 1.8 Å. Population parameters (p) for each of these peaks were refined by least-squares procedures on the basis that each atom was an "average atom" with an atomic scattering curve of $(f_{Na^+} + f_{Nb^{5+}})/2$. The pentagonal holes each with a single atom occupancy refined to $p = 0.37(02)$, that is 8.51 ± 1.5 electrons, i.e., one sodium ion. The central atom of the triplet refined to $p = 0.35(02)$, that is 8.05(46) electrons with each end member of each triplet refining to $p = 0.14(01)$ or 3.5(2) electrons. Each triplet is, therefore, one $3Na^+/4$ plus two $Nb^{5+}/8$. The composition of the sodium niobium bronze is $Na_{13}Nb_{35}O_{94}$ and this agrees well with the $Na_2O:Nb_2O_5$ molar ratio of 1:3 from which the compound was made. The calculated density, ρ_c, of 4.64 gcm^{-3} is also in better agreement with ρ_{obsd}(= 4.62 gcm^{-3}) than those values previously suggested.

Atomic parameters were refined by full-matrix least-squares procedures to yield the values listed in Table I. The reliability index R for the 1651 observed data is 0.045, and these data are on deposit.[1]

[1] For detailed paper, extended version, or supplementary material, order NAPS Document 01217 from ASIS National Auxiliary Publications Service, c/o CCM Information Sciences, Inc., 22 West 34th Street, New York, New York 10001; remitting \$2.00 for microfiche or \$5.00 for photocopies.

TABLE I

ATOMIC PARAMETERS FOR $Na_{13}Nb_{35}O_{94}$

Atom	x/a	y/b	z/c	$\beta_{11} \times 10^5$	$\beta_{22} \times 10^5$	$\beta_{33} \times 10^4$	$\beta_{12} \times 10^5$	$\beta_{13} \times 10^5$	$\beta_{23} \times 10^5$
Nb(1)	0.5000	0.000	0.5000	163(15)	16(1)	629(36)	1(3)	0	0
Nb(2)	0.07993(12)	0.7091(4)	0.5315(18)	122(9)	11(1)	258(16)	5(2)	−15(47)	8(14)
Nb(3)	0.02141(12)	0.17327(4)	0.5020(18)	92(9)	13(1)	1005(21)	−5(2)	−61(61)	−67(19)
Nb(4)	0.21835(13)	0.30877(4)	0.5131(18)	136(9)	15(1)	361(18)	−4(2)	−86(53)	32(16)
Nb(5)	0.07520(13)	0.40313(4)	0.5189(19)	99(8)	16(1)	591(22)	1(2)	50(68)	8(19)
Nb(6)	0.29842(14)	0.13814(4)	0.5012(1)	114(9)	20(1)	657(24)	4(2)	−58(70)	40(23)
Nb(7)	0.42699(15)	0.23379(4)	0.4971(19)	294(12)	14(1)	428(23)	−4(3)	−17(70)	12(19)
Nb(8)	0.29553(14)	0.47814(4)	0.52848(19)	123(8)	11(1)	356(18)	−1(2)	−23(52)	−6(15)
Nb(9)	0.33769(13)	0.39054(4)	0.4318(17)	101(8)	12(1)	125(12)	2(2)	−1(30)	−1(10)
Nb(10)	0.2910(11)	0.1910(4)	−0.0053(77)	67(93)	3(10)	−22(130)	23(21)	−89(43)	−61(136)
Nb(11)	0.0861(14)	0.2660(4)	−0.0009(81)	150(115)	19(13)	360(176)	29(26)	454(540)	51(176)
Na(1)	0.00000	0.00000	0.0092(71)	331(84)	61(10)	283(150)	−24(23)	0	0
Na(2)	0.0061(11)	0.3330(3)	0.0069(72)	774(91)	64(8)	772(140)	15(23)	977(521)	446(147)
Na(3)	0.3333(14)	0.0553(4)	0.0102(80)	1063(136)	112(16)	881(208)	137(35)	−683(757)	−67(214)
Na(4)	0.1843(20)	0.2261(7)	−0.0051(86)	1837(273)	276(40)	854(216)	564(88)	−705(961)	−43(336)
O(1)	0.11002(78)	0.01893(27)	0.05113(57)	115(59)	8(6)	457(95)	8(15)	−90(315)	−26(98)
O(2)	0.22175(84)	0.09106(28)	0.4929(57)	86(60)	13(7)	428(99)	−1(16)	271(321)	179(104)
O(3)	0.00288(83)	0.11800(29)	0.4813(54)	121(63)	12(6)	212(109)	−2(16)	588(289)	111(95)
O(4)	0.16783(88)	0.16500(27)	0.4732(52)	148(58)	22(6)	1017(102)	13(16)	−370(334)	40(90)
O(5)	0.02142(85)	0.22341(28)	0.4806(55)	189(57)	17(6)	588(101)	27(16)	537(311)	−33(95)
O(6)	0.34026(83)	0.00307(28)	0.4947(55)	138(66)	22(7)	460(98)	20(16)	−365(373)	25(92)
O(7)	0.44762(84)	0.12411(28)	0.4973(51)	140(61)	13(6)	629(95)	25(15)	−42(323)	−163(97)
O(8)	0.35678(81)	0.18945(28)	0.4922(51)	129(59)	14(6)	629(91)	−3(16)	126(309)	−6(95)
O(9)	0.29241(84)	0.26259(28)	0.4885(56)	230(58)	23(6)	235(104)	17(16)	276(314)	−63(104)
O(10)	0.07089(117)	0.29340(39)	0.4687(99)	156(85)	27(10)	618(226)	−17(24)	539(603)	172(188)
O(11)	0.36448(105)	0.33481(36)	0.4921(115)	104(72)	18(9)	996(247)	−1(22)	−476(651)	364(218)
O(12)	0.18622(81)	0.36325(26)	0.4752(49)	−14(64)	7(7)	353(101)	1(16)	114(291)	−131(92)
O(13)	0.21922(102)	0.42935(34)	0.4875(76)	81(79)	11(9)	482(157)	8(20)	−90(437)	−153(154)
O(14)	0.00106(87)	0.44776(28)	0.4573(56)	232(64)	14(7)	824(109)	12(16)	−121(286)	11(92)
O(15)	0.41717(80)	0.44088(26)	0.5028(54)	86(60)	10(6)	391(91)	−6(16)	139(331)	11(106)
O(16)	0.00000	0.50000	−0.0209(131)	642(230)	226(45)	695(256)	201(79)	0	0
O(17)	0.08318(84)	0.06973(29)	−0.0064(80)	204(67)	34(6)	262(109)	−7(16)	155(324)	−39(101)
O(18)	0.02819(86)	0.17620(28)	−0.0126(71)	710(59)	53(6)	85(113)	17(15)	461(321)	6(102
O(19)	0.21431(83)	0.30788(28)	−0.0208(74)	321(58)	35(6)	158(122)	8(17)	−380(310)	86(99)
O(20)	0.07566(83)	0.40260(28)	0.0036(73)	314(58)	69(6)	323(98)	45(17)	−43(336)	−65(97)
O(21)	0.30313(89)	0.14759(28)	−0.0211(61)	545(63)	69(7)	100(117)	−59(16)	−259(289)	73(86)
O(22)	0.43238(84)	0.23397(28)	−0.0168(70)	411(63)	55(6)	18(117)	51(16)	−562(326)	49(104)
O(23)	0.30049(141)	0.47944(45)	−0.0106(101)	503(114)	47(13)	351(173)	−33(31)	−230(495)	−42(164)
O(24)	0.33867(88)	0.39005(29)	−0.0297(74)	139(58)	28(6)	260(130)	11(16)	12(274)	−82(86)

[a] Standard deviations are given in brackets and refer to the least significant places of the preceding number. The thermal parameters are of the form $T = \exp[-10^{-4}(\beta_{11}h^2 + \beta_{22}k^2 + \beta_{33}l^2 + 2\beta_{12}hk + 2\beta_{13}hl + 2\beta_{23}kl)]$.

Pertinent bond distances within each coordination polyhedron are given in Table II.

Description of the Structure

The structure of $Na_{13}Nb_{35}O_{94}$ consists of a continuous host matrix of corner-sharing niobium–oxygen octahedra in which every four- and five-sided tunnel is occupied by interstitial ions (see Fig. 1). In general, the niobium atom of each octahedron is displaced up to 0.12 Å, in the same sense, away from the (002) basal plane of the octahedron. The oxygen atoms comprising the basal planes are all displaced in the same, but opposite sense away from the (002) plane. The structure therefore has a [001] polar axis.

TABLE II

BOND DISTANCES (Å) WITHIN THE COORDINATION POLYHEDRA WHICH CONSTITUTE THE ASYMMETRIC PART OF THE UNIT CELL

Nb(1) *Octahedron*	
Nb(1)–O(6)[1]	1.978(12)
Nb(1)–O(6)[4]	1.978(12)
Nb(1)–O(14)	1.940(12)
Nb(1)–O(14)[2]	1.940(12)
Nb(1)–O(16)	2.060(61)
Nb(1)–O(16)[6]	1.895(61)
O(14)–O(6)[1]	2.839(18)
O(6)[1]–O(14)[2]	2.699(17)
O(14)[2]–O(6)[4]	2.839(18)
O(6)[4]–0(14)	2.699(17)
O(16)–O(14)	2.704(46)
O(16)–O(6)[1]	2.841(47)
O(16)–O(14)[2]	2.704(46)
O(16)–O(6)[4]	2.841(47)
O(16)[6]–O(14)	2.827(47)
O(16)[6]–O(6)[1]	2.754(46)
O(16)[6]–O(14)[2]	2.827(47)
O(16)[6]–O(6)[4]	2.754(46)
Nb(2) *Octahedron*	
Nb(2)–O(1)	1.960(12)
Nb(2)–O(2)	1.973(13)
Nb(2)–O(3)	1.995(13)
Nb(2)–O(15)[4]	2.062(12)
Nb(2)–O(17)	2.128(37)
Nb(2)–O(17)[6]	1.829(37)
O(1)–O(2)	3.037(17)
O(2)–O(3)	2.947(17)
O(3)–O(15)[4]	2.424(16)
O(15)[4]–O(1)	2.810(16)
O(17)–O(1)	2.799(35)
O(17)–O(1)	2.773(35)
O(17)–O(3)	2.810(32)
O(17)–O(15)[4]	2.902(34)
O(17)[6]–O(1)	2.698(33)
O(17)[6]–O(2)	2.777(36)
O(17)[6]–O(3)	2.878(34)
O(17)[6]–O(15)[4]	2.852(33)
Nb(3) *Octahedron*	
Nb(3)–O(3)	2.059(13)
Nb(3)–O(4)	1.840(13)
Nb(3)–O(5)	1.857(12)
Nb(3)–O(11)[4]	1.964(15)
Nb(3)–O(18)	2.040(32)
Nb(3)–O(18)[6]	1.924(32)
O(3)–O(4)	2.680(17)
O(4)–O(5)	2.819(17)
O(5)–O(11)[4]	2.899(20)
O(11)[4]–O(3)	2.445(18)
O(18)–O(3)	2.924(30)
O(18)–O(4)	2.616(31)
Nb(3) *Octahedron—cont.*	
O(18)–O(5)	2.620(33)
O(18)–O(11)[4]	2.872(47)
O(18)[6]–O(3)	2.956(30)
O(18)[6]–O(4)	2.699(32)
O(18)[6]–O(5)	2.660(33)
O(18)[6]–O(11)[4]	2.846(44)
Nb(4) *Octahedron*	
Nb(4)–O(9)	1.941(13)
Nb(4)–O(10)	1.918(18)
Nb(4)–O(11)	2.049(16)
Nb(4)–O(12)	2.059(11)
Nb(4)–O(19)	2.112(34)
Nb(4)–O(19)[6]	1.845(34)
O(9)–O(11)	2.817(20)
O(11)–O(12)	2.443(19)
O(12)–O(10)	2.951(20)
O(10)–O(9)	2.968(21)
O(19)–O(9)	2.792(34)
O(19)–O(10)	2.679(44)
O(19)–O(11)	2.925(46)
O(19)–O(12)	2.857(31)
O(19)[6]–O(9)	2.740(33)
O(19)[6]–O(10)	2.740(46)
O(19)[6]–O(11)	2.855(46)
O(19)[6]–O(12)	2.879(31)
Nb(5) *Octahedron*	
Nb(5)–O(12)	2.023(12)
Nb(5)–O(13)	2.031(15)
Nb(5)–O(14)	1.904(13)
Nb(5)–O(7)[4]	1.874(13)
Nb(5)–O(20)	2.038(34)
Nb(5)–O(20)[6]	1.917(34)
O(12)–O(13)	2.479(18)
O(13)–O(14)	2.785(20)
O(14)–O(7)[4]	2.744(17)
O(7)[4]–O(12)	2.988(17)
O(20)–O(12)	2.732(29)
O(20)–O(13)	2.792(37)
O(20)–O(14)	2.620(31)
O(20)–O(7)[4]	2.701(32)
O(20)[6]–O(12)	2.890(31)
O(20)[6]–O(13)	2.880(38)
O(20)[6]–O(14)	2.883(33)
O(20)[6]–O(7)[4]	2.737(33)
Nb(6) *Octahedron*	
Nb(6)–O(2)	1.952(12)
Nb(6)–O(7)	1.916(13)
Nb(6)–O(8)	2.031(12)
Nb(6)–O(4)	1.899(13)
Nb(6)–O(21)	2.067(28)
Nb(6) *Octahedron—cont.*	
Nb(6)–O(21)[6]	1.890(28)
O(2)–O(7)	2.988(16)
O(7)–O(8)	2.665(17)
O(8)–O(4)	2.506(16)
O(4)–O(2)	2.833(17)
O(21)–O(2)	2.824(31)
O(21)–O(7)	2.765(30)
O(21)–O(8)	2.871(28)
O(21)–O(4)	2.766(29)
O(21)[6]–O(2)	2.746(30)
O(21)[6]–O(7)	2.658(29)
O(21)[6]–O(8)	2.797(28)
O(21)[6]–O(4)	2.797(29)
Nb(7) *Octahedron*	
Nb(7)–O(8)	1.856(12)
Nb(7)–O(10)[3]	2.047(17)
Nb(7)–O(5)[3]	1.968(13)
Nb(7)–O(9)	1.976(13)
Nb(7)–O(22)	2.034(32)
Nb(7)–O(22)[6]	1.924(32)
O(8)–O(10)[3]	2.724(20)
O(10)[3]–O(5)[3]	2.661(21)
O(5)[3]–O(9)	2.879(18)
O(9)–O(8)	2.821(18)
O(22)–O(8)	2.764(31)
O(22)–O(10)[3]	2.765(44)
O(22)–O(5)[3]	2.751(32)
O(22)–O(9)	2.848(31)
O(22)[6]–O(8)	2.713(30)
O(22)[6]–O(10)[3]	2.846(43)
O(22)[6]–O(5)[3]	2.766(32)
O(22)[6]–O(9)	2.819(32)
Nb(8) *Octahedron*	
Nb(8)–O(13)	2.042(15)
Nb(8)–O(15)	2.042(12)
Nb(8)–O(1)[1]	1.909(12)
Nb(8)–O(6)[1]	1.919(12)
Nb(8)–O(23)	2.119(47)
Nb(8)–O(23)[6]	1.839(47)
O(13)–O(15)	2.485(18)
O(15)–O(1)[1]	2.907(16)
O(1)–O(6)[1]	2.907(17)
O(6)[1]–O(13)	2.825(19)
O(23)–O(13)	2.885(44)
O(23)–O(15)	2.871(41)
O(23)–O(1)[1]	2.760(43)
O(23)–O(6)[1]	2.790(41)
O(23)[6]–O(13)	2.895(45)
O(23)[6]–O(15)	2.796(40)
O(23)[6]–O(1)[1]	2.633(40)
O(23)[6]–O(6)[1]	2.761(43)

TABLE II—*continued*

Nb(9) *Pentagonal Bipyramid*		*Na*(1) *Square Prism—cont.*		*Na*(4) *Trigonal Prism*	
Nb(9)–O(11)	2.101(16)	Na(1)–O(15)[10]	3.137(27)	Na(4)–O(18)	2.670(23)
Nb(9)–O(12)	2.134(12)	Na(1)–O(1)[8]	2.494(32)	Na(4)–O(21)	3.588(39)
Nb(9)–O(13)	2.063(16)	Na(1)–O(15)[9]	3.137(27)	Na(4)–O(22)	3.082(31)
Nb(9)–O(15)	2.124(12)			Na(4)–O(19)	2.725(38)
Nb(9)–O(3)[3]	2.076(12)	*Na*(2) *Square Prism*		Na(4)–O(22)[4]	3.448(3)
Nb(9)–O(24)	1.825(34)	Na(2)–O(19)	2.738(19)	Na(4)–O(5)	2.785(40)
Nb(9)–O(24)[6]	2.130(34)	Na(2)–O(22)[4]	2.641(20)	Na(4)–O(4)	2.954(38)
O(11)–O(3)[3]	2.445(18)	Na(2)–O(21)[4]	2.738(20)	Na(4)–O(8)	3.222(41)
O(3)[3]–O(15)	2.424(16)	Na(2)–O(20)	2.715(20)	Na(4)–O(9)	2.725(38)
O(15)–O(13)	2.485(18)	Na(2)–O(10)	2.474(43)	Na(4)–O(10)	3.418(48)
O(13)–O(12)	2.479(18)	Na(2)–O(8)[4]	2.790(30)	Na(4)–O(5)[7]	2.864(39)
O(12)–O(11)	2.443(19)	Na(2)–O(7)[4]	2.609(33)	Na(4)–O(4)[7]	3.066(38)
O(24)–O(11)	2.922(46)	Na(2)–O(12)	3.105(30)	Na(4)–O(8)[7]	3.215(42)
O(24)–O(3)[3]	2.880(31)	Na(2)–O(10)[7]	2.705(46)	Na(4)–O(9)[7]	2.761(40)
O(24)–O(15)	2.986(32)	Na(2)–O(8)[9]	2.871(33)	Na(4)–O(10)[7]	3.536(49)
O(24)–O(13)	2.912(38)	Na(2)–O(7)[9]	2.665(32)		
O(24)[6]–O(11)	2.802(48)	Na(2)–O(12)[7]	3.261(27)		
O(24)[6]–O(3)[3]	—	*Na*(3) *Trigonal Prism*		*Nb*(10) *Square Pyramid*	
O(24)[6]–O(15)	2.810(31)	Na(3)–O(16)[3]	2.906(16)	Nb(10)–O(21)	1.983(21)
O(24)[6]–O(13)	2.818(37)	Na(3)–O(20)[3]	3.378(25)	Nb(10)–O(22)	2.363(20)
O(24)[6]–O(12)	2.893(30)	Na(3)–O(21)	3.071(22)	Nb(10)–O(4)	2.613(34)
		Na(3)–O(17)	3.139(22)	Nb(10)–O(8)	2.130(40)
Na(1) *Square Prism*		Na(3)–O(23)[5]	3.257(29)	Nb(10)–O(4)[7]	2.738(35)
Na(1)–O(17)	2.778(13)	Na(3)–O(14)[3]	2.728(33)	Nb(10)–O(8)[7]	2.148(41)
Na(1)–O(23)[5]	2.583(20)	Na(3)–O(7)	3.493(31)		
Na(1)–O(17)[2]	2.778(13)	Na(3)–O(2)	2.668(37)		
Na(1)–O(23)[4]	2.583(20)	Na(3)–O(1)	3.654(33)	*Nb*(11) *Square Pyramid*	
Na(1)–O(1)	2.507(33)	Na(3)–O(6)	2.721(35)	Nb(11)–O(19)	2.217(24)
Na(1)–O(15)[5]	3.105(27)	Na(3)–O(14)[11]	3.016(37)	Nb(11)–O(22)[4]	1.902(24)
Na(1)–O(1)[2]	2.507(33)	Na(3)–O(7)[7]	3.550(33)	Nb(11)–O(10)	2.123(54)
Na(1)–O(15)[4]	3.105(27)	Na(3)–O(2)[7]	2.768(36)	Nb(11)–O(5)	2.599(36)
Na(1)–O(1)[7]	2.494(32)	Na(3)–O(1)[7]	3.650(31)	Nb(11)–O(10)[7]	2.337(55)
		Na(3)–O(6)[7]	2.809(35)	Nb(11)–O(5)[7]	2.708(38)

[a] Standard deviations are in brackets; superscripts denote the following symmetry transformations of the parameters in Table I:

[No superscript]	x	y	z
1	$\frac{1}{2}-x$	$\frac{1}{2}+y$	z
2	$\bar{x}$	$\bar{y}$	z
3	$\frac{1}{2}+x$	$\frac{1}{2}-y$	z
4	$x-\frac{1}{2}$	$\frac{1}{2}-y$	z
5	$\frac{1}{2}-x$	$y-\frac{1}{2}$	z
6	x	y	$z+1$
7	x	y	$z-1$
8	$\bar{x}$	$\bar{y}$	$z-1$
9	$x-\frac{1}{2}$	$\frac{1}{2}-y$	$z-1$
10	$\frac{1}{2}-x$	$y-\frac{1}{2}$	$z-1$
11	$\frac{1}{2}-x$	$\frac{1}{2}-y$	$z-1$

The three-sided tunnels, which are large enough to hold small cations such as Li^+ (*15*), are too small to hold the larger Na^+ and Nb^{5+} ions. An atom at the centre of the trigonal prism is surrounded by nine oxygen neighbors each at approximately 2.2 Å, and this distance is considerably less than the sum of the oxygen and sodium ionic radii (2.67 Å) after corrections have been made for the increased

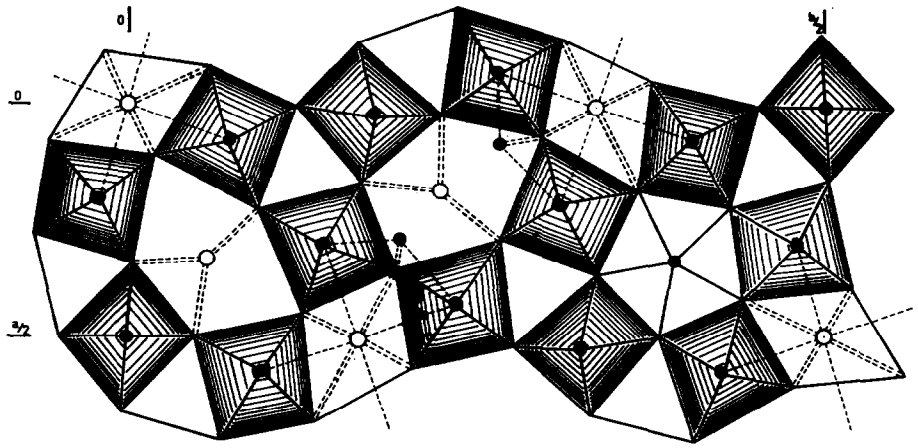

FIG. 1. An (001) projection of the structure of the asymmetric unit of $Na_{13}Nb_{35}O_{94}$. Niobium atoms are shown as filled circles; open circles represent sodium ions. Dotted lines show the nearest oxygen approaches to sodium ions and to the square pyramidal niobium atoms. Double lines are directed to oxygen ions which are separated by one c translation and which therefore overlap in this projection.

coordination number. Although the Nb–O equilibrium distance is of the order of 2 Å, it is probable that such bonds are covalent and therefore directional. The symmetry of the coordination polyhedra presented to a niobium atom situated in the three-sided tunnels is incompatible with the directional properties of the bonding orbitals of niobium(V).

All four-sided tunnels are filled with sodium ions so that each is surrounded by 12 nearest oxygen atoms. Equilibrium Na–O distances range between 2.50 and 3.26 Å. The bordering Nb–O octahedra are not unduly distorted by these filled four-sided tunnels, since the sodium and niobium cations lie at different levels along c. However, there is some movement of the apical oxygen atoms from their ideal positions due to an electrostatic attraction to the sodium ion (at the same level along c).

The remaining sodium ions are located in five-sided tunnels but these are significantly distorted and the coordination about each sodium can best be described in terms of a trigonal prism (Na–O, 2.7 Å) with additional oxygen atoms locatedthrough the rectangular prism faces (Na–O, 3.2–3.6 Å).

Four of the 12 pentagonal tunnels in the unit cell are filled with niobium and oxygen atoms, each niobium atom having a pentagonal bipyramidal coordination polyhedron. The pentagon is extremely regular; O–O distances within the basal plane vary between 2.424(16)–2.485(18) Å while the distances of these five oxygen atoms from the apical oxygen atoms vary between 2.810(31)–2.986(32) Å. Niobium–oxygen distances [1.825(34)–2.134(12) Å] are slightly larger than those in the octahedra. The niobium atom is displaced 0.15 Å from the basal plane of the pentagonal bipyramid but in the opposite direction to similar displacements in the octahedra. The five octahedra bordering each five-sided tunnel are distorted in that each central metal atom is displaced from the centre of its octahedron due to repulsion by the seven-coordinated metal atom. The edge which forms one of the pentagonal sides is also unusually short ($\approx$2.45 Å).

The remaining four pentagonal tunnels are again filled and contain sodium and niobium ions in the ratio 3:1. Sodium ions, Na(4), are located approximately in the (001) planes and occupy a central position similar to that described above. Six oxygen ions form a trigonal prism about each Na(4) and lie at distances of $\approx$2.7 Å with the remaining oxygen atoms located through the rectangular prism faces at slightly longer distances. Niobium atoms Nb(10) and Nb(11) are located in the (001) planes but are displaced from the central polygon position towards the surrounding oxygen atoms. This displacement may occur in either of two equally probable directions, each of which allows the niobium atoms to form directional bonds with certain oxygen atoms. The distances listed in Table II indicate that, for each niobium atom Nb(10) and Nb(11), the nearest neighbours at Nb–O distances of 2.1 Å are arranged as the base of a square pyramid.

Discussion

Four of the 12 five-sided tunnels in this structure are fractionally occupied with sodium and niobium atoms. In other tetragonal-bronze structures where fractional occupancy has been observed (*7*) it was

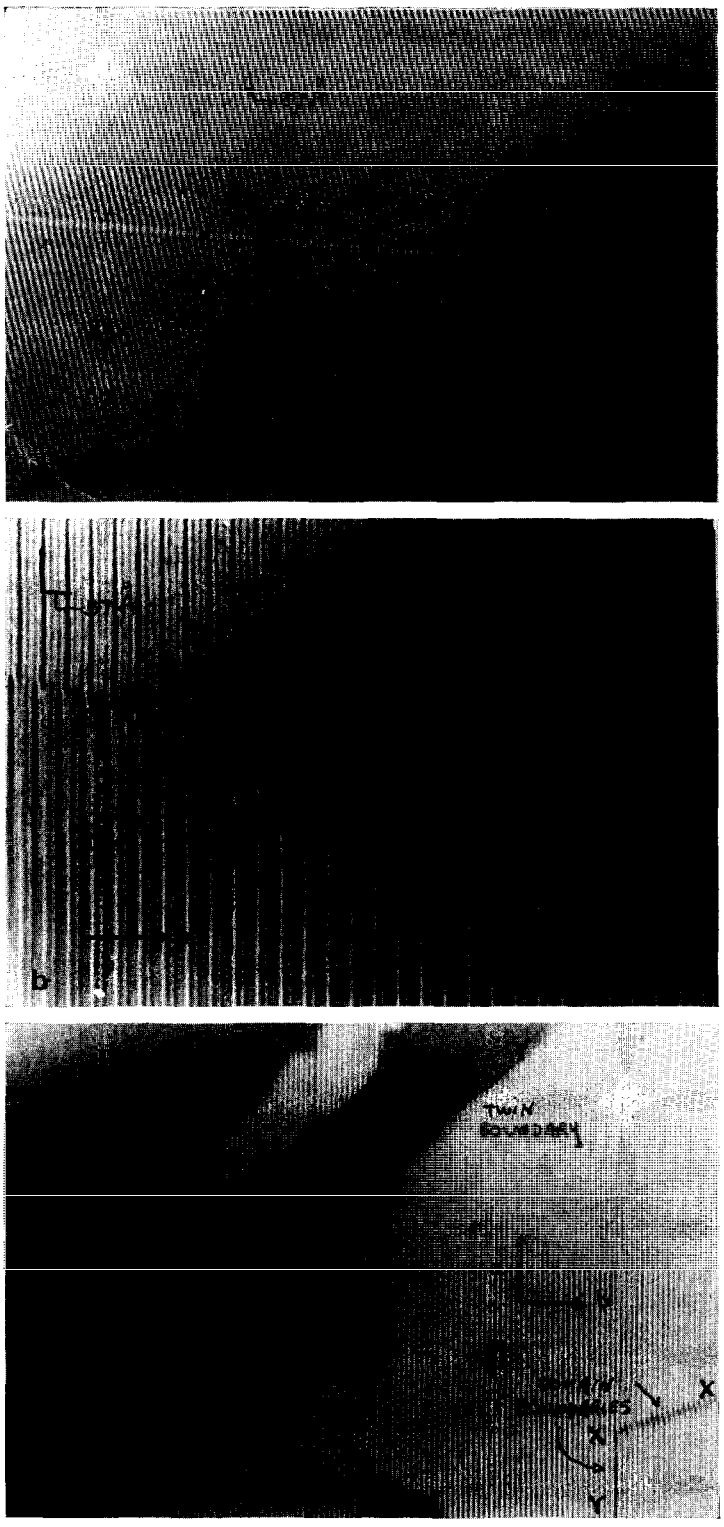

FIG. 2. Electron transmission micrographs of thin crystals of $Na_{13}Nb_{35}O_{94}$ using $0k0$ reflections. (a) A domain boundary, $x - x$, inclined at $18\frac{1}{2}°$ to the [010] direction. There is a slip of $b/3$ Å at the domain boundary. The parallel fringes are spaced at 37 Å, which corresponds to the b axis of the unit cell. Magnification: 316,000×. (b) Magnification: 1,160,000×. The tetragonal bronze subcell can be seen as faint lines between the heavy fringes. The displacement between adjacent domains is one subcell. (c) Domain boundaries $x - x$, inclined at $18\frac{1}{2}°$ to the [010] direction and $x - y$, which are parallel to the [100] direction. A twin boundary is shown as $T - T$. Magnification: 260,000×.

postulated that this was a result of the formation of microdomains of ordered regions, *of different compositions*, which are formed during the annealing process at temperatures where diffusion is reasonably rapid. Electron transmission micrographs of the compound $Na_{13}Nb_{35}O_{94}$ were, therefore, taken in order to determine whether the fractional occupancy can be explained in terms of microdomain formation. Figure 2(a)–(c) shows lattice image photographs of selected areas of thin edges of crystals of $Na_{13}Nb_{35}O_{94}$ and these were very kindly taken by Dr. J. G. Allpress, Tribo Physics, C.S.I.R.O., Melbourne. The parallel fringes in Fig. 2(a) are spaced at ≈ 37 Å, which corresponds to the *b* axis of the unit cell. At the domain boundary, Fig. 2(a) and (b), it is quite clear that the unit cell is shifted by one third of this *b* axis, i.e., by one tetragonal subcell. The domain boundaries are either inclined by $18\frac{1}{2}°$ to the *b* axis, Fig. 2(a) and (b), or run parallel to the *a* axis, Fig. 2(c).

In general, the domain boundaries are considerable distances apart and the microdomains which they separate are of mosaic block-size and therefore diffract as single entities. Within each domain the lattice fringes are quite regularly separated with no evidence of any planar faulting. If adjacent domains are of different composition, then, based upon the structural evidence, the most likely compositions are $Na_{14}Nb_{34}O_{94}$ and $Na_{10}Nb_{38}O_{94}$. The former composition corresponds to an ordering of sodium ions in the holes characterized by fractional occupancy while the latter corresponds to an ordering of niobium ions in these holes. These compositional regions would be required to occur in the ratio 3:1 and, in addition, these regions would be charged since the compositions are not ionically compensated. In view of the large and approximately equally sized domains found in the areas imaged by electron transmission it seems most likely that domains are of the same composition and that the one niobium and three sodium atoms are statistically distributed over the four tunnels available for them in each unit cell of $Na_{13}Nb_{35}O_{94}$.

The questions then arises: Why do these large unfaulted and compositionally identical domains interface at a domain boundary with either a slip of one tetragonal subcell at $18\frac{1}{2}°$ to the *b* axis or along the *a* axis? One explanation is that the domains are in fact ferroelectric domains oriented in antipolar directions along the [001] axis. It can be shown below that the *b*/3 slip and the finite domain boundaries are a result of the distortions introduced into the continuous host matrix by a change in polarity of the crystal structure.[2]

[2] An alternative model has been proposed (*16*) in which adjacent domains differ only in the manner in which four and five sided tunnels are filled. The host matrix is continuous throughout the crystal and out-of-phase boundaries, which do not have finite width, arise when domains meet on (110) planes.

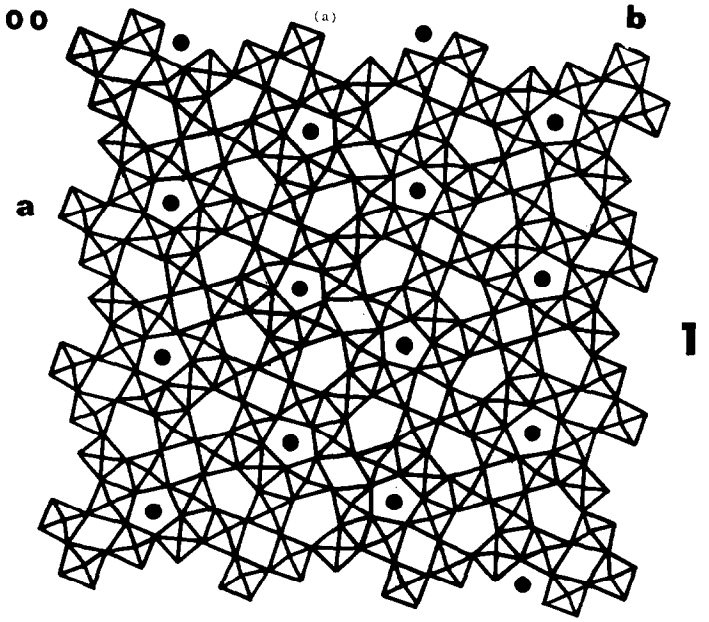

FIGURE 3 (a)

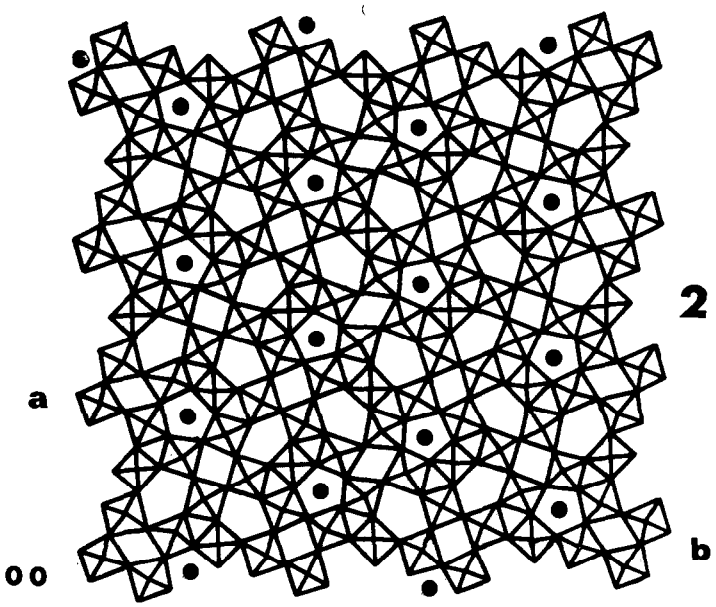

FIGURE 3 (b)

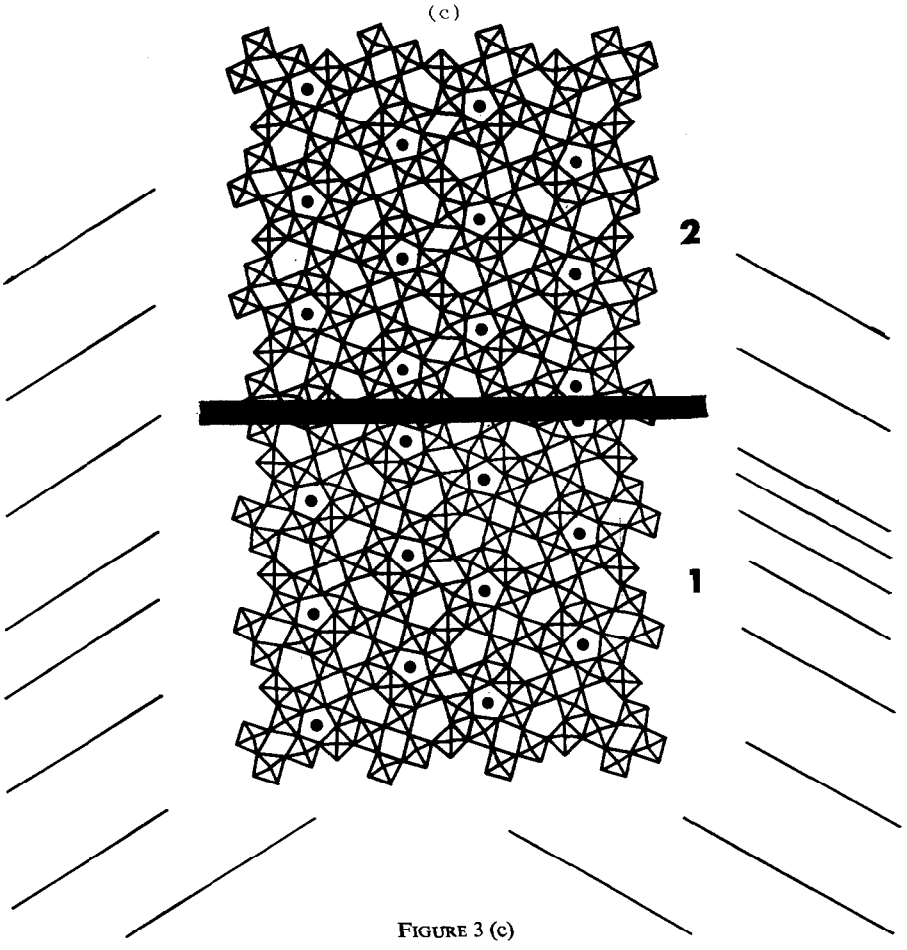

FIGURE 3 (c)

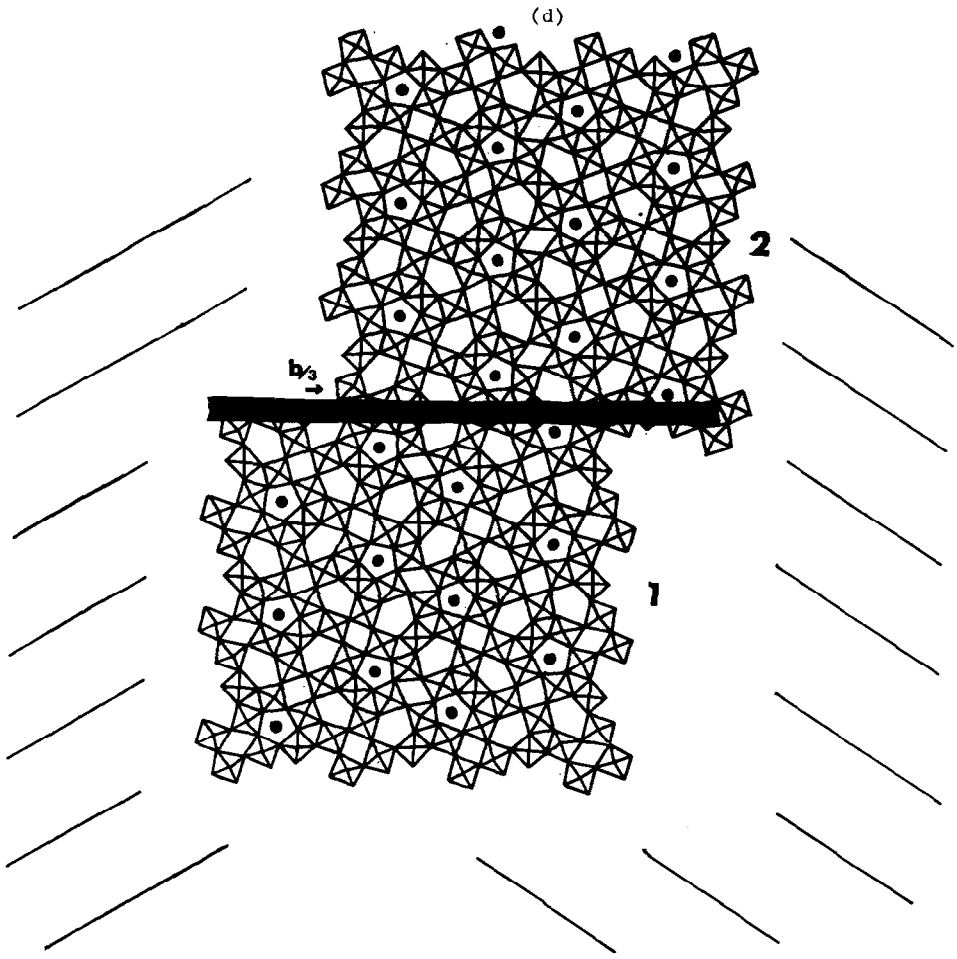

FIGURE 3 (d)

Ferroelectric Domains and Domain Boundary Orientation

Figure 3 depicts a block (1) of three unit cells of the compound $Na_{13}Nb_{35}O_{94}$. The five-sided tunnels that are completely filled with Nb–O strings of atoms are marked with heavy dots, while the sodium atoms have been omitted for clarity. The heavy dots are packed in hexagonal close array. If this block is now rotated 180° about a twofold axis parallel to [010] the block (2) shown in Fig. 3(b) is obtained. Transmission micrographs using the oko set of reflections will be identical for both blocks and consist of parallel fringes separated by ≈ 37 Å. If the blocks are interfaced as in Fig. 3(c) the lattice images of the blocks will be continuous but the structural features over the two blocks will not be regular. If may be possible to rearrange the octahedra at the interface so that the host matrix exhibits continuity through both blocks. However, the black dots, which may be taken as representing charge distribution in the four- and five-sided tunnels, do not show a continuous hexagonal close packing over *both* blocks.

A translation along the *b* axis of one tetragonal bronze subcell, shown in Fig. 3(d) does produce the desirable symmetry in the distribution of black dots over the double block.

Super lattices arise in the T.T.B. structures by the manner in which the four- and five-sided tunnels are filled with interstitial ions. Because of this, each tetragonal bronze subcell is not *exactly* equivalent to its adjacent neighbour, but nevertheless the continuous host matrix of corner sharing octahedra maintains an approximate periodicity of one tetra-

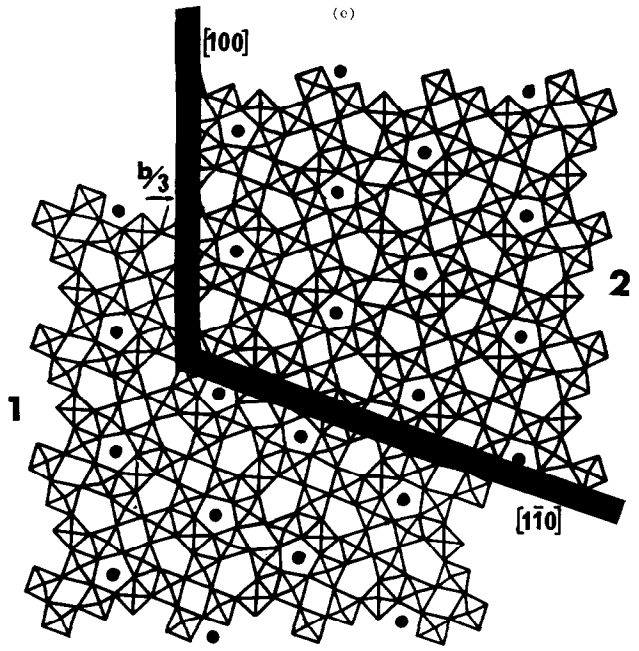

FIGURE 3 (e)

FIG. 3. (a) A block (1) of unit cells of the compound $Na_{13}Nb_{35}O_{94}$. The five-sided tunnels that are completely filled with Nb–O strings of atoms are marked with heavy dots, which are in close-packed hexagonal array. (b) A block (2) of 3 unit cells, related to block (1) by a twofold axis parallel to [010]. (c) The direct interface of block (1) and block (2). The close-packed hexagonal array of black dots is not continuous over the whole structure, as shown by the irregular distances between planes of dots. The domain boundary between blocks (1) and (2) is shown as a heavy black line. (d) The interfacing of block (1) and block (2) involving a translation of one block by $b/3$ Å. There is now a regular close packing of black dots over the whole of the structure, as shown by a regular spacing between planes of dots. (e) Adjacent domains (blocks) interface along (1$\bar{1}$0) and (010) planes. This arrangement is shown here. At the actual interface (heavy black lines) adjustments must be made to atomic positions so that a regular continuum of the corner sharing octahedra, as well as filled tunnels, occurs throughout the crystal.

gonal bronze subcell. The one subcell displacement along b therefore results in

1. A continuity of the host matrix through blocks (1) and (2).
2. The same symmetry of stacking of the Nb–O pentagonal bipyramids and the double block as that existing in each separate block.
3. The same stacking arrangement of the sodium filled tunnels over the double block as that existing in each separate block. (This arises because all four-sided and $87\frac{1}{2}\%$ of the remaining five-sided tunnels in each subcell are filled with sodium ions.)

The double block can therefore be regarded essentially as a continuum. The change in polarity of one block with respect to the other does, however, cause distortions, which are sufficient to produce changes in the continuity of the lattice fringes. The structure of adjacent domains are related as twins except that in addition, a displacement of $b/3$ occurs at the composition plane.

Adjacent domains interface along the (1$\bar{1}$0) plane, which is inclined at $18\frac{1}{2}°$ to the b axis. A finite boundary extends from this plane into each domain and this boundary domain may measure up to 38 Å [Fig. 3(a)] in width. This upper limit may be an over-estimate. The crystal used for transmission micrographs is slightly tilted and the domain boundary image is really a projection of a boundary with finite width. Within this domain there is a slight and gradual reorientation of each octahedron so that the host matrix of one ferroelectric domain may change smoothly into the host matrix of the adjacent antipolar domain. The thickness of the domain walls as measured from transmission micrographs agrees well with estimates made by Känzig and Sommerhalder (*17*) from wall energies and by Merz (*18*, *19*) from observations made with a

polarizing microscope. These workers estimated the domain boundaries to be one to three unit cells in thickness.

It has been shown that the individual domains are large enough to diffract as single entities. Superimposed on the *hkl* spots from one domain will be the $hk\bar{l}$ spots from an adjacent antipolar domain. Although these data need not necessarily have the same phase, the structure amplitudes do have the same magnitudes and, therefore, the data collected over one-eighth of the reciprocal lattice will be representative of the asymmetric unit of reciprocal space diffracted by one domain. The structure, as deduced from these data, has shown that each domain possesses polarity along [001] and should therefore exhibit the characteristics of a line ferroelectric.

Acknowledgment

We are indebted to Dr. J. G. Allpress for taking and providing the electron transmission micrographs shown in Fig. 2.

References

1. S. Andersson, *Acta Chem. Scand.* **19**, 557 (1965).
2. A. Reisman, F. Holtzberg, and E. Banks, *J. Amer. Chem. Soc.* **80**, 37 (1958).
3. M. W. Shafer and R. Roy, *J. Amer. Ceram. Soc.* **42**, 482 (1959).
4. S. Andersson, *Acta Crystallogr. Sect. A* **16**, 21 (1963).
5. C. D. Whiston and A. J. Smith, *Acta Crystallogr.* **19**, 169 (1965).
6. N. C. Stephenson, *Acta Crystallogr.* **18**, 496 (1965).
7. N. C. Stephenson, *Acta Crystallogr. Sect. B* **24**, 637 (1968).
8. D. C. Craig and N. C. Stephenson, *Acta Crystallogr. Sect. B* **25**, 2071 (1969).
9. W. R. Busing and H. A. Levy, *Acta Crystallogr.* **22**, 457 (1967).
10. W. Hoppe, *Agnew. Chem.* **77**, 484 (1965).
11. A. Magneli, *Ark. Kemi.* **1**, 213 (1949).
12. T. Suzuki, *Acta Crystallogr.* **13**, 279 (1960).
13. D. T. Cromer and J. T. Waber, *Acta Crystallogr.* **18**, 104 (1965).
14. C. H. Dauben and D. H. Templeton, *Acta Crystallogr.* **8**, 841 (1955).
15. J. J. Rubin, L. G. Van Uitert, and H. J. Levinstein, *Int. J. Cryst. Growth* (1968).
16. J. G. Allpress, Private Communication.
17. W. Känzig and R. Sommerhalder, *Helv. Phys. Acta.* **26**, 603 (1953).
18. W. Merz, *Phys. Rev.* **88**, 421 (1952).
19. W. Merz, *Phys. Rev.* **95**, 690 (1954).
20. W. R. Busing, K. O. Martin, and H. A. Levy, ORFLS, USAEC Report ORNL-TM-305.
21. W. R. Busing, K. O. Martin, and H. A. Levy, ORFFE, USAEC Report ORNL-TM-306.